

INTEGRATION OF AIRBORNE AND CARBORNE GAMMA RAY SPECTROMETRIC SURVEYS, WADI ELGIDAMI AREA, CENTRAL EASTERN DESERT, EGYPT

I.M. Gaafar, K.G. Ali and M.I. Mira

Nuclear Materials Authority, P. O. Box 530, Maadi, Cairo, Egypt

تكامل المسح الإشعاعي الجوى الطيفى والمسح الأرضى فى منطقة وادي الجدامي بوسط وشرق الصحراء الشرقية فى مصر

الخلاصة: تهدف الدراسة الحالية إلى تفسير نتائج المسح الإشعاعي الطيفى الجوى وبالسيارة ومدى التوافق بينهما لمنطقة وادي الجدامي والمناطق المحيطة بوسط الصحراء الشرقية لمصر. وقد أسفرت الخرائط الناتجة عن وجود توافق كبير بين بيانات كل من المسح الإشعاعي الجوى وتلك الناتجة عن مسح السيارة. حيث يتميز جرانيت المسيكات الواقع بشمال شرق المنطقة بارتفاع المحتوى الإشعاعي للعناصر الثلاث البوتاسيوم (٥,٦%) واليورانيوم (٣٠ جزء فى المليون) والثوريوم (٦٠ جزء فى المليون). كما أن الجزء الغربى للمنطقة والذي تغطيه مكونات الداخلة الرسوبية التى تحتوى على طبقات الفوسفات الحاملة لليورانيوم يصل فيه تركيز اليورانيوم إلى أكثر من ٤٢ جزء فى المليون دون أى زيادة ملحوظة لكل من البوتاسيوم (٠,٣%) والثوريوم (٢ جزء فى المليون) عن الخلفية الإشعاعية المنخفضة لهذه الصخور. أما باقى صخور المنطقة المحيطة والمتمثلة فى صخور الجرانيت القديم وباقى الصخور الرسوبية بالمنطقة فتعبر عن مستوى اشعاعى ضعيف ولا تحتوى أى تغيرات ملحوظة. وإيضاح المقارنة بين كل من نتائج المسح الإشعاعي الجوى ونتائج المسح الإشعاعي الأرضى فقد تم دراسة بروفييل يقطع منطقة الدراسة من الجنوب الغربى فى اتجاه الشمال الشرقى والذي أظهر وجود توافق كبير للغاية بينهما. وتوضح الخريطة المجمع لليورانيوم ونسبه التوافق على شاذتين عاليتين إحداهما فى الجنوب الغربى والأخرى فى الشمال الغربى وهو الأكبر اتساعا والأعلى فى القيمة والأهم كمصدر لليورانيوم وربما الفوسفات كذلك. بينما يظهر جرانيت المسيكات الحديث أنه يحتوى على تركيز عال نسبيا لليورانيوم ولكن يحتوى على قيم قليلة لكل من اليورانيوم/الثوريوم وكذلك اليورانيوم/البوتاسيوم وهذا يعنى أن خلفيته الإشعاعية عالية بطبيعتها ويقبل من أهميته كمصدر لليورانيوم. ومن هنا توصى الدراسة بعمل مسح جيولوجى وجيوفيزيائى حقلى تفصيلى للجزء الشمالى الغربى من المنطقة وتجميع عينات ممثلة لدراستها كيميائيا بغرض تقييم محتواها من اليورانيوم وإمكانية استغلالها.

ABSTRACT: Qualitative interpretation was executed on the airborne and car-borne spectrometric data of Wadi Elgidami area and its surroundings, Central Eastern Desert, Egypt. Elmissikat younger granites are characterized by increase in the three main radioactive elements; up to 5.6% K, 30 ppm eU and 60 ppm eTh and found in the eastern part of the study area. The western part of the study area includes Dakhla Formation which contains uranium-bearing phosphate beds. They are characterized by increase of uranium up to 42 ppm without potassium or thorium enrichment. Radioactivity level decreases strongly in older granites and the surrounding country rocks. Stacked profiles were used to correlate the three radioelements and their ratios for both airborne and car-borne data. It was found that the radioelement profiles of airborne data agree well with that obtained by car-borne survey. Both of them show that phosphates are the dominant rocks that effectively contribute to eU anomalies, occurring in the study area. The three-dimensional and composite image maps for eU and (eU/eTh) reveal that there are two important anomalies, in the younger granitic rocks, located in the southwestern and northwestern parts of the study area; both are connected to the Dakhla Formation, which contains phosphate beds. The northwestern anomaly seems to represent the highest one in the study area and, hence, is considered very important from the eU point of view and needs more detailed studies.

1. INTRODUCTION

Wadi Elgidami study area is located in the Central Eastern Desert of Egypt between latitudes 26° 17' 30"N - 26° 30' 30"N and longitudes 33° 01' 30"E- 33° 25' 30"E (Fig. 1). It is covered by different varieties of rock formations, including successions of basement and sedimentary rocks. The contact zone between both is considered as an unconformity. The area under consideration was included in an airborne gamma-ray spectrometric survey which was conducted 1984. Meanwhile, the car-borne spectrometric data were conducted by the car-borne system of Nuclear Materials Authority, in 2012. The present study deals with the interpretation of these airborne and car-borne

spectrometric survey data. In this study, the geological map of the study area was considered as a base for the radiometric lithologic interpretation of the spectrometric data.

The ability of gamma-ray spectrometry to map potassium, uranium, and thorium enrichment or depletion provides powerful exploration guidance in a wide variety of geological settings. In this study, the airborne and car-borne gamma-ray spectrometric survey data were interpreted and integrated. Besides, the composite image technique was used to display simultaneously three parameters including three radioelement concentrations and their ratios on one image. The technique offered

much in terms of lithologic discrimination based on colour differences and showed efficiency in defining areas where different lithofacies occur within areas mapped as one continuous lithology.

The airborne gamma-ray spectrometric method is widely used in diverse fields. Initially it was developed as uranium exploration, geological mapping (Ammar, 1973; Anderson and Nash, 1997; Graham, and Bonham-carter, 1993; Jaques et al., 1997; Charbonneau et al., 1997; Gaafar, 2005; IAEA, 2010), mineral exploration (Grasty and Shives, 1997; Lo and Pitcher, 1996), soil mapping (Cook et al., 1996; Wilford et al., 1997), and environmental radiation monitoring (Lahti et al., 2001; Ford et al., 2001; Sanderson et al., 1995).

Car-borne gamma-ray spectrometry was used for source search (Ulvsand et al., 2002; Hjerpe et al., 2001), contamination surveying and mapping (Moreira, 1991; Hovgaard, 1997; Karlsson et al., 2000; Sanderson et al., 2003) and prospecting (Grasty and Cox, 1997). Variations in the radioactivity of rocks may be useful for geological mapping (Aissa and Jubeli, 1997), for acquiring information on the distribution of radiation exposure rates (Raghuwanshi, 1992), and for environmental monitoring (Tauchid and Jubeli, 1991). Total gamma radioactivity can be used by health physicists for acquiring information on the distribution of radiation exposure rates (Raghuwanshi, 1992), and a car-borne radiometric system can be effectively used for an emergency response action due to radioactive incident or contamination (Tauchid and Jubeli, 1991).

2. GEOLOGICAL SETTING

The study area is covered by a variety of basement and sedimentary rocks, ranging in age from Precambrian to Quaternary (Fig. 1). Precambrian rocks cover the eastern part of the study area and comprise ophiolites, metavolcanics, older granites and younger granites. Meanwhile, the upper Cretaceous Nubian sandstones cover the central part of the area and are represented by Taref Formation. In the western and northwestern parts of the area, Late Cretaceous shale and limestone are represented by Dakhla, Dawi and Qusseir Formations (Conoco Report, 1989). The following is a field description of these rocks and their main associated geologic feature carried out by the authors of this work:

2.1. Basement complex:

2.1.1. Ophiolitic mélanges:

They are represented by serpentinites, metagabbros, and basalt to the south east of the study area. Serpentinites form conspicuous mountainous ridges with steep slopes, while metagabbros are represented by small masses, medium-grained, highly altered, deformed, and occasionally foliated.

2.1.2. Metavolcanics

Metavolcanics form low hills at the southern part of the study area (Fig. 1). They are composed of fine to

medium-grained meta-andesites and metabasalts. Sometimes, they are found as xenoliths in the granites.

2.1.3. Older granites:

Older granites are represented by separated low-relief hills intruded by younger granites and dykes, with sharp contacts. They have whitish to grayish colours and are more or less heterogeneous, that range from tonalitic to granodioritic composition. The grain size varies from medium to coarse-grained and sometimes displays gneissic texture and exfoliation. They are mainly composed of plagioclase, quartz, little K-feldspar, hornblende and biotite, with epidote, titanite (sphene) and iron oxides as accessory minerals.

2.1.4. Felsic dyke swarm:

The area also comprises a phase of granitic magma represented by a dyke swarm striking in an ENE to NE direction, which seems to be reactivated many times. These dykes extend for about 10 km in length, but with variable widths. They comprise aplite and porphyry dykes. Field relations indicated that aplite dykes cut older granite only, whereas porphyry dykes seem to cut all younger granite phases.

2.1.5. Younger granites

Younger granites in the area are important rocks as they host U-mineralized silica veins. They crop out as concentric oval bodies extending in a NW-SE directions and are bounded by and traversed with several NW-SE and ENE-WSW trending faults and wadis (Fig. 1). They form the highest peaks in the study area as Gabal El-Missikat and Gabal El-Gidami. Generally, they can be categorized with high potassium leucogranite zoned plutons. They are mainly composed of potash feldspar, smoky quartz, and plagioclase with biotite and accessory fluorite crystals. The background contents of radioelement in these granites are unusually higher than expected and increase towards the inner zone.

2.2. Foreland "Cover" sediments:

Three main sedimentary types can be seen unconformably overlying the peneplained surface of the Precambrian basement complex to the west of the area under investigation. These sediments represent a considerable succession ranging in age from Cretaceous to Quaternary.

2.2.1. Taref formation (Nubian sandstones):

In the central part of the study area, basement rocks are unconformably overlain by a sequence of continental to shallow marine tabular cross-bedded sandstones. They are nearly horizontal beds and extend westwards, where they finish up to an upper sequence of marine variegated shales, limestones and phosphorites near Gabal Abu Had (Duwi formation) of late Cretaceous age (Said, 1962). So, it is considered of early Cretaceous as assigned to similar formations of Nubian Sandstones.

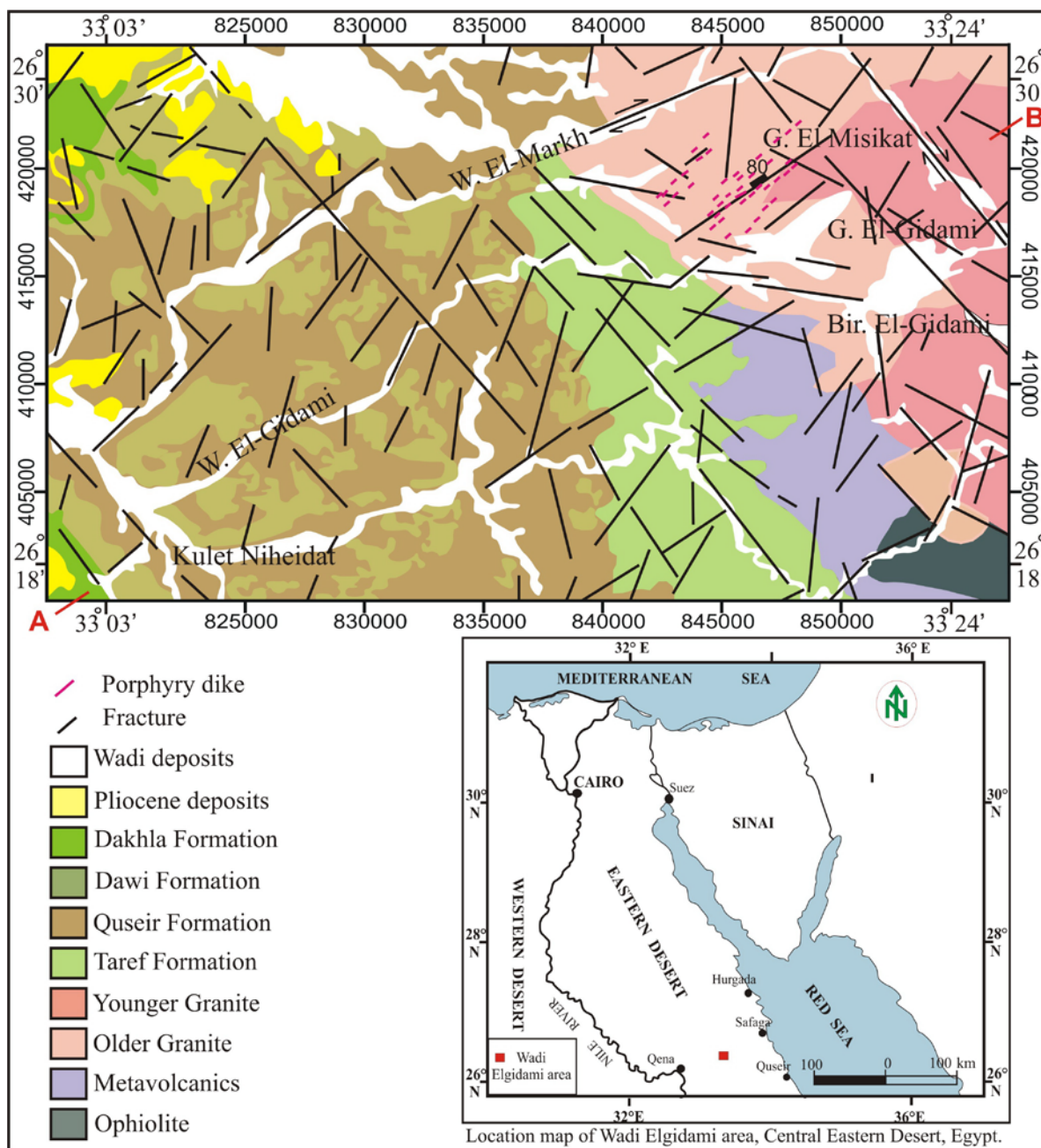


Fig. (1) Geologic map of Wadi Elgidami area, Central Eastern Desert, Egypt. A-B the direction of profile in Figures 14&15.

Nubian Sandstones in the study area get their importance from their age, which may be contemporaneous to some of the U-mobility stages, and from being a lateral extension sedimentary basin along the main mineralized shear zone in the granite (Ibrahim, 2002).

2.2.2. Quseir formation (Variegated shale):

Variegated shales consist of multicoloured shale (grey, brownish yellow, green, reddish, violet and blackish) alternating with yellowish sandstone at Gebel Duwi. The upper part of the Quseir Variegated shales contains some phosphate bands. So, the upper part of

this formation is very similar to the shale lithofacies of the Duwi formation (Glenn and Mansour 1979).

2.2.3. Duwi formation (Phosphate-bearing sediments):

This formation is characterized by the presence of three types of sections: a clay section, a sandy-clay section and a sandy section (Ghanem, et al., 1970). Three phosphate-bearing members: lower, middle and upper are recognized in this formation. The phosphate beds could be considered as a probable source of uranium, where their average content reaches 130 ppm. Besides, phosphates have an average P₂O₅ content reaching 13.5% (Salman, 1970).

2.2.4. Dakhla formation (Chalk formation):

This formation is represented at the base of Dakhla formation. There occurs a horizon composed of phosphatic limestones, which grade laterally to phosphorites (Ghanem, et al., 1970). It is mainly represented by chalky limestone and marl which some authors define them as the Chalk Formation (Said, 1962).

2.2.5. Paleocene sediments:

Paleocene sediments conformably overlie Dakhla Formation. They are represented in the study area by thin-laminated greenish marl and clayey limestone at the base, and thin-laminated marl and greenish clayey limestone at the top (Ghanem, et al., 1970).

2.2.6. Quaternary sediments:

They are represented by alluvial and proluvial loams, sands, muds and conglomerates along the main Wadis.

3. AIRBORNE SPECTROMETRIC SURVEY DATA

Airborne gamma-ray spectrometric data were acquired, in 1984 by Aero Service, over the Eastern Desert of Egypt including the study area. The survey was flown using fixed-wing aircraft equipped with a high-sensitivity 256-channel airborne gamma-ray spectrometer system. The survey was carried out along a set of parallel flight lines maintaining 1.0 km line spacing and NE-SW direction. Nominal sampling interval and flight height were 90 m and 120 m terrain clearance, respectively (Aero Service, 1984).

The data were corrected for background radiation resulting from cosmic rays and aircraft contamination, variations caused by changes in aircraft altitude relative to ground, and Compton scattered gamma rays in potassium and uranium energy windows. The corrected data provide an estimate of the apparent surface concentrations of potassium, equivalent uranium, and equivalent thorium (K, eU, and eTh). The data were gridded at 50 m intervals, prior to producing colour images for the three radioelement concentrations, their ratios as well as radioelement colour composite images.

4. CARBORNE SPECTROMETRIC SURVEY DATA

Car-borne gamma-ray spectrometric system is composed of a GR-320 portable multichannel gamma-ray spectrometer with a large volume scintillation detector. The position for each measurement point is determined by a GPS instrument, while its latitude and longitude, as well as measured γ -ray spectrometric data are collected by a computer. The complete system, loaded in a field car, was used for radioactive mineral exploration after calibration by NMA pads. A lot of data confirm that the system works stably and reliably, and is a fast and advanced approach for radioactive mineral γ -ray spectrometric exploration. It can be used not only to determine the contents of natural radioactive elements in the environment, but also to monitor nuclear

pollution and emergency treatment in nuclear accidents significantly.

5. RESULTS

Gamma-ray spectrometry provides a direct measurement of the surface distribution of the naturally occurring radioelements (K, U, and Th). Potassium is a major constituent of most rocks, while uranium and thorium are present in trace amounts, as mobile and immobile elements, respectively. As the concentrations of these radioelement vary between different rock types, the measured radioelement distribution can be reliably used to map and distinguish the different lithologies (IAEA, 2010).

5.1. K (%) Distribution:

Airborne potassium distribution map (Fig. 2) shows that the eastern side of the study area is characterized by the highest concentration of up to 5.6% that is associated mainly with younger granites. Meanwhile, potassium contents up to 2.5% are associated with older granites and aplite dykes, which surround younger granites in the northeastern part of the study area. Sedimentary rocks, at some parts of Dawi formation possess potassium concentrations reaching 2%. Meanwhile, metavolcanics, ophiolites, basic rocks and Dakhla formation show the lowest concentrations in the study area reaching less than 0.5%, which is located in the southeastern and western parts of the study area, respectively. These results are confirmed by car-borne potassium distribution map (Fig. 3), which describes the gradual increase of potassium from the southwest, where Dakhla formation is located, to the northeastern direction which is associated with younger granites.

5.2. eTh (ppm) Distribution:

Equivalent thorium distribution map (Fig. 4) represents the background radiation for most rocks of the study area, with the exception of younger granites, which are characterized by the highest eTh values in the area, reaching up to 60 ppm, which represents three the average content of they are granites in nature. Older granites come within the second level, where their eTh concentration reaches about 7 ppm, but located in the natural level of radiation. It is clear that the remaining rocks of the study area display low eTh content. They show significant lateral variations that distinguish each rock unit from the others. This level is no longer relevant and is located within the background radiation, which does not represent any radiological risk to the environment. Dawi formation is characterized by relative eTh (5 ppm) increments than the surrounding rocks that take irregular forms and often trend in the northwest-southeast direction. Meanwhile, ophiolites, metavolcanics and Dakhla formation represent the lowest eTh concentrations in the study area. Car-borne eTh distribution map (Fig. 5) shows high agreement with airborne eTh distribution map (Fig. 4). On this map, younger granites are characterized by the highest eTh concentrations in the study area which reach also 60 ppm.

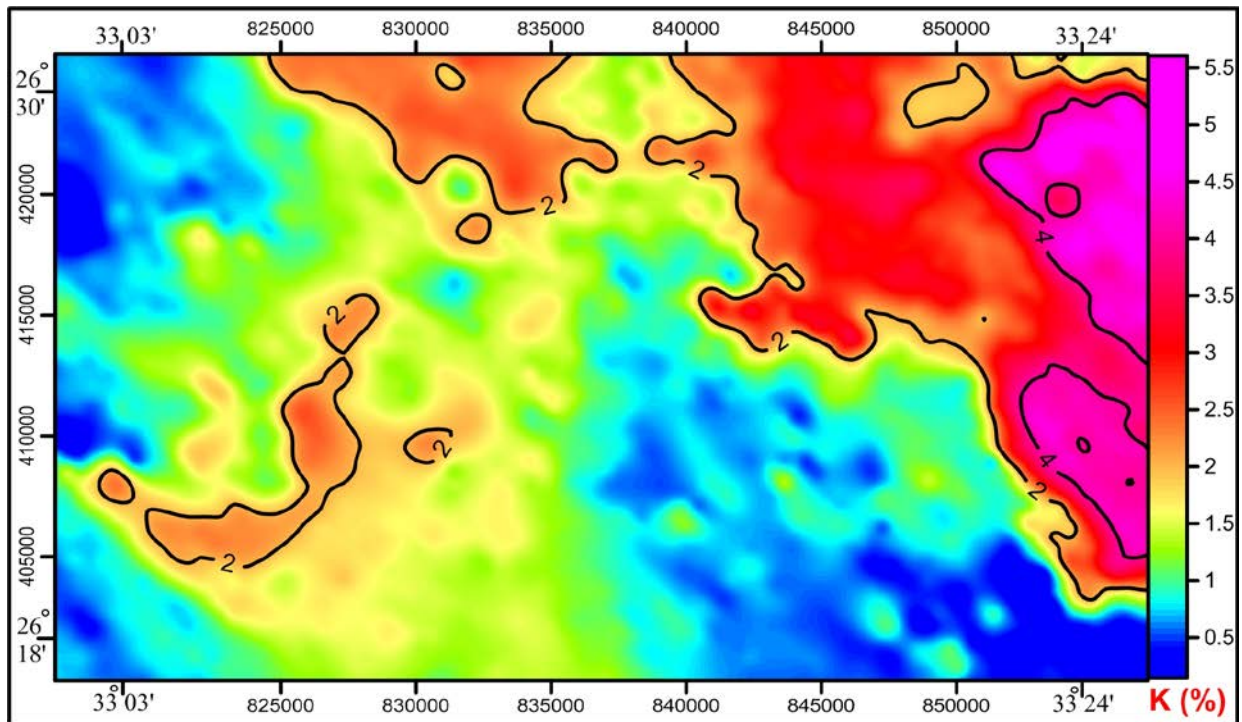


Fig. (2): Airborne K (%) image map of Wadi Elgidami area, Central Eastern Desert, Egypt.

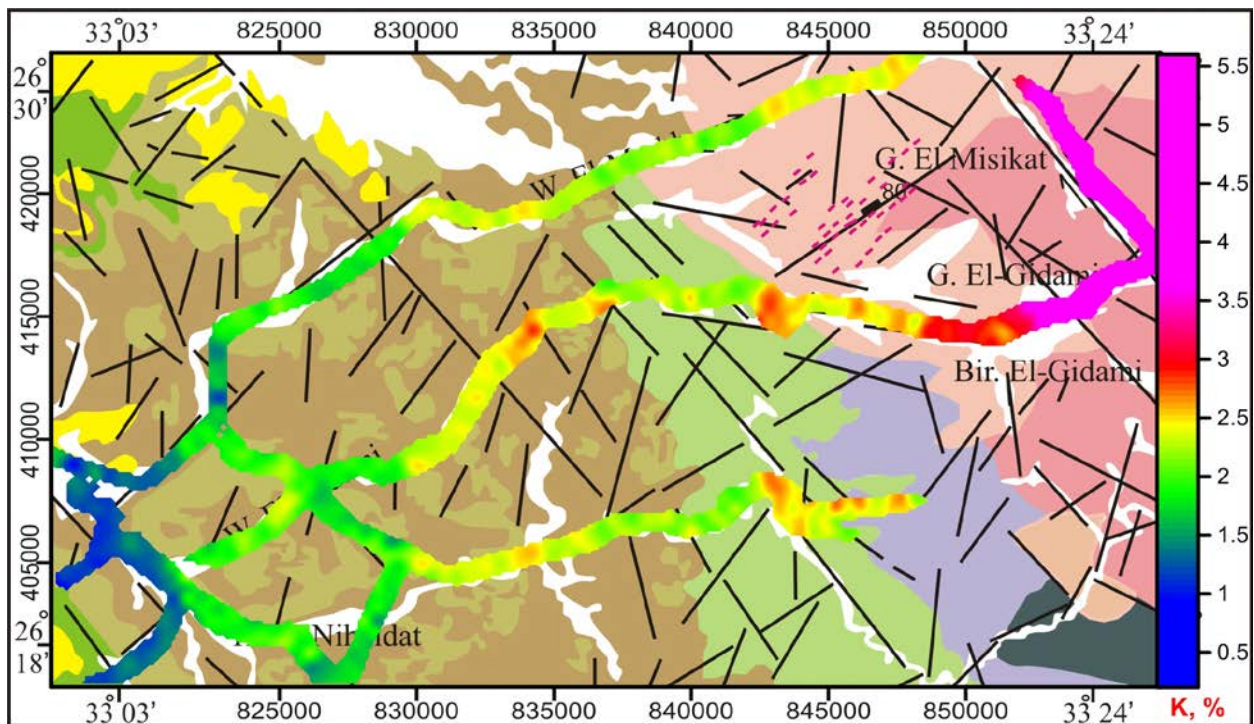


Fig. (3): Car-borne K (%) image map of Wadi Elgidami area, Central Eastern Desert, Egypt.

5.3. eU (ppm) Distribution:

The study of the distribution of the equivalent uranium (eU) in the study area shows clearly that its level ranges from less than 1 ppm to 45 ppm (Fig. 6). Phosphates that are located in the western part of the study area are characterized by the highest eU concentrations. One of these anomalies takes a semi-circular form in the northwestern corner of the study area and the other is located in its southwestern corner and is elongated in the northwestern direction. Younger granites represent the second level which is located in the northeastern part of the study area and its highest concentration reaches 30 ppm. Meanwhile older granites and Dawi formation come in the third level which takes random forms that are linked largely with nearby rocks and represent the lowest level of eU content. Basement rocks and their country rocks, located in the southeastern part of the study area, show eU content reaching less than 2 ppm and extend in a north northwestern direction.

Comparing airborne and car-borne eU distribution maps (Figs 6 & 7) reflect a clear agreement, in which phosphates are characterized by the highest content of eU than younger granites. Meanwhile, the remaining rocks reflect normal content, and do not represent any significant increase.

6. DISCUSSION

6.1. Three-Dimensional Images

Study of the distribution of radioactive elements on the three-dimensional image maps indicates that both distributions of airborne K and airborne eTh maps (Figs. 8 & 9) are linked to younger granites in the northeastern part of the study area, while the rest of the area represents the background radiation of crustal rocks. According to the three-dimensional image map of airborne eU (Fig. 10), it is clear that there are three main anomalous zones. The first anomalous zone is located in the northeastern part of the study area and is associated with Elmissikat younger granites. The second anomalous zone is located to the southwestern part of the study area is related to the phosphates. The third anomalous zone is located in the northwestern part of the study area that might be connected to the Dakhla formation and perhaps also to phosphates.

Meanwhile, the eU/eTh 3D image map (Fig. 11) shows that there are two important anomalies which are located in the southwestern and northwestern of the study area. Both anomalies are related to the Dakhla formation, which contains phosphates. These two eU/eTh anomalies represent the most important and significant zones in the investigated area, because of their association with phosphates and with the lowest level of both K and eTh concentrations.

6.2. Airborne Composite Images:

With the advances in computer-image processing technology, different methods of representing, displaying and processing radiometric data were

developed. The basis of this technology is the representation of radiometric data in a digital raster format, which contains both amplitude (colour) and spatial information. Composite images provide a simultaneous display of up to three parameters on one image and facilitates the correlation and delineation of areas based on subtle differences in numerical values. The following combinations are developed by United States of Geological Survey (USGS) (Duval, 1983); 1. The radioelement composite image combines the data of K (in red), eTh (in green), and eU (in blue), 2. The uranium composite image combines the data of eU (in red) with the ratios eU/eTh (in green) and eU/K (in blue).

Obviously, there is often good correlation between the geological map and composite image maps of radioactive elements (Figs. 1 & 13). Younger granites are characterized by an increase of the radioactivity content of the three radioactive elements so, they appear white in colour. Then, the radioactivity contents of the three elements decrease gradually westwards due to the low-land younger granites, which are characterized by yellow-white colour. Radioactivity content and, hence, uranium and thorium elements decreases strongly in older granites, adjacent to younger ones, which are characterized by pale red colour as a result of the predominance of potassium. Wadi sediments appear yellow in colour, which reflects the level of background radiation for the three radioactive elements in the study area. Clearly, the lowest level of radiation in the study area is associated with basic rocks in its southeastern part, which takes a dark black colour, then metavolcanics, which appear in dark red mixed with black. Radiation level, increases slightly in Taref formation which is characterized by a mix of dark blue and green, black colours. Meanwhile Dawi and Quseir formations appear on the geological map as inter-bedded in large sections of the central and western parts, but on the study area, composite image map, they could be divided it into two parts. The first part occupies the central and southern parts of the studied area, which appear slightly high in radioactivity and show a mixture of bright colours of yellow, green, red and blue. The other part, which occupies the western part of the study area, possesses low radiation and shows the same colours but darks. The western part of the study area includes Dakhla formation which includes uranium-bearing phosphate beds. These deposits are characterized by an increase of uranium, without potassium or thorium and therefore, their colours are bright blue.

Composite image map of eU and its two ratios shows two high anomalies that are distinguished by white colour. The first anomaly is located in the southwestern and the other one in the northwestern parts of the study area (Fig. 13). The latter anomaly is the most significant and higher in value might represent a source of uranium and possibly it is phosphate as well.

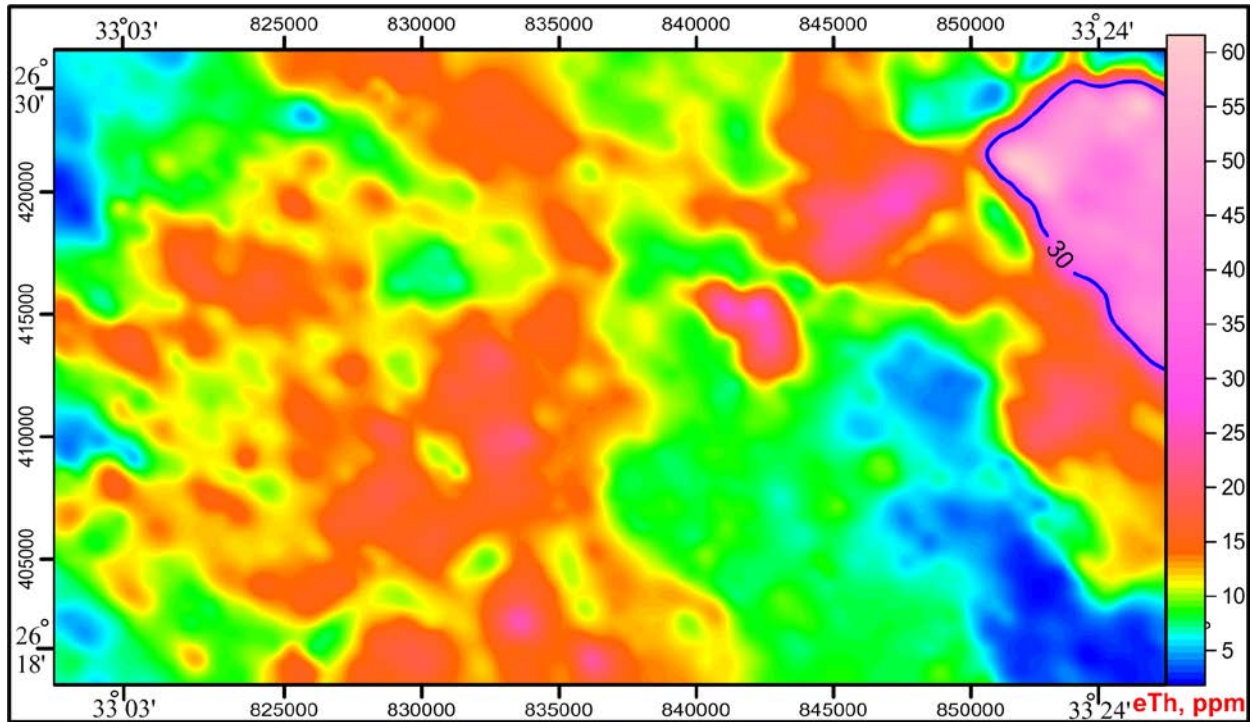


Fig. (4) Airborne eTh (ppm) image map of Wadi Elgidami area, Central Eastern Desert, Egypt.

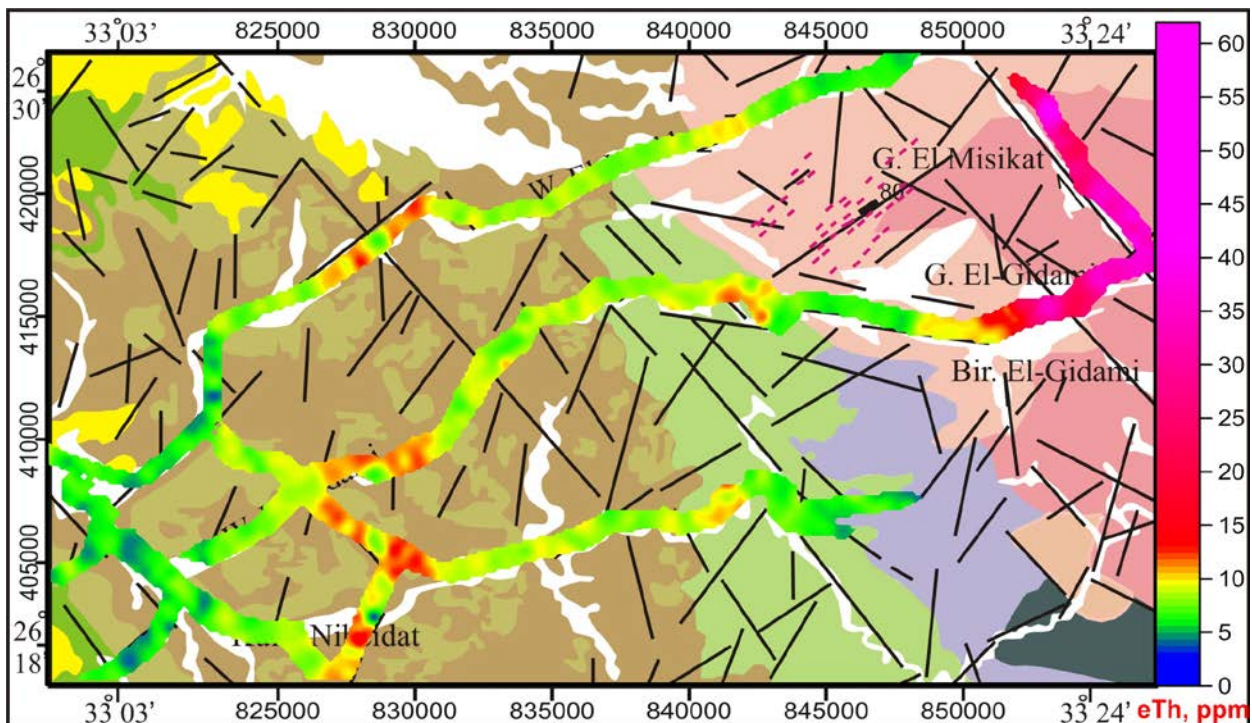


Fig. (5) Car-borne eTh (ppm) image map of Wadi Elgidami area, Central Eastern Desert, Egypt.

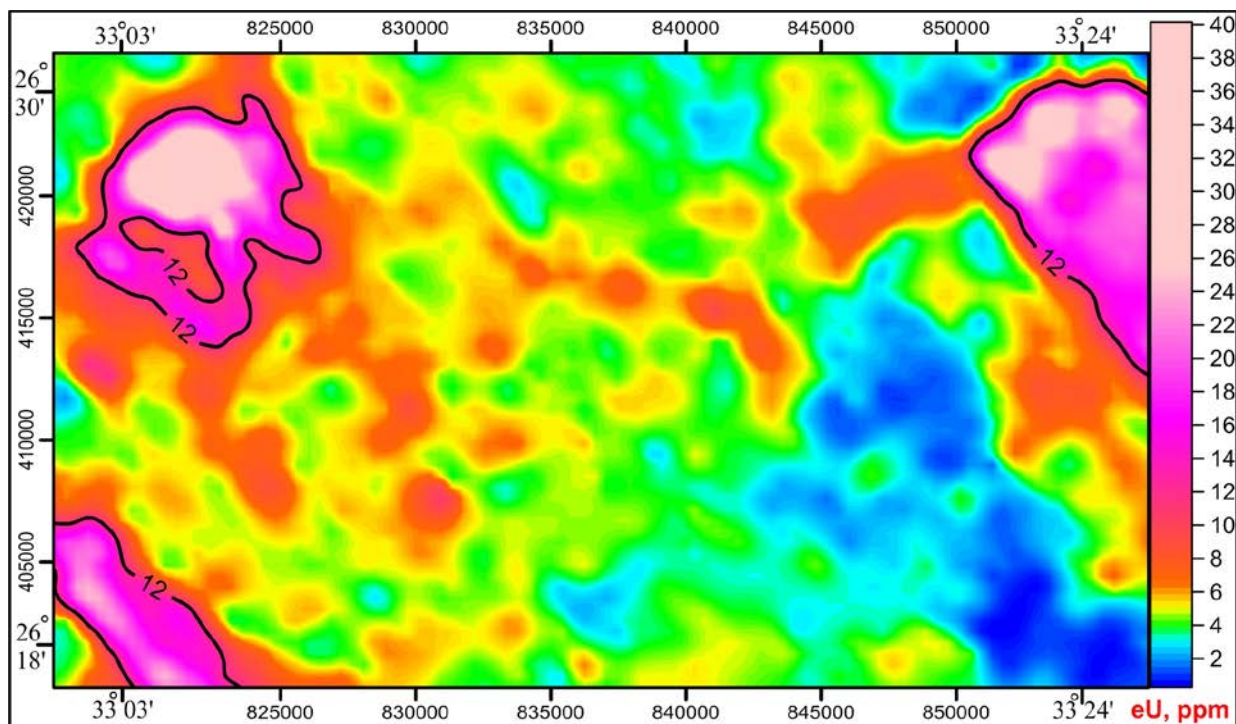


Fig. (6) Airborne eU (ppm) image map of Wadi Elgidami area, Central Eastern Desert, Egypt.

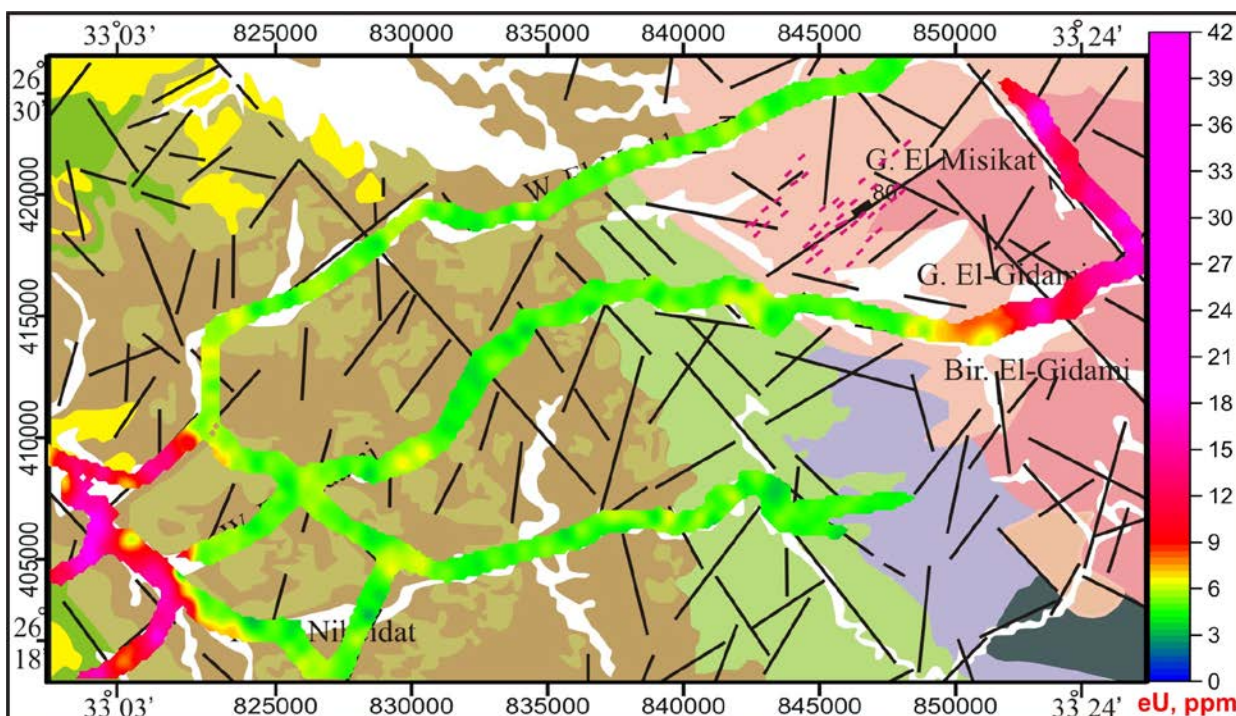


Fig. (7) Car-borne eU (ppm) image map of Wadi Elgidami area, Central Eastern Desert, Egypt.

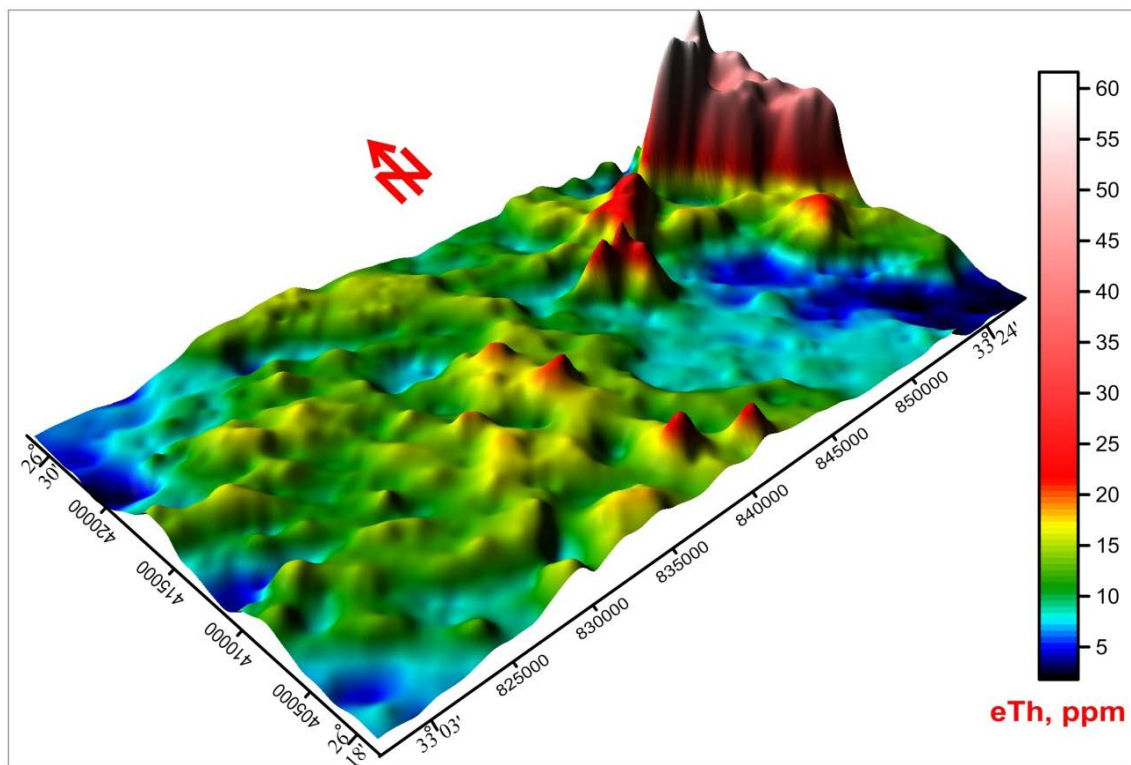


Fig. (8): Airborne eTh (ppm) 3D image map of Wadi Elgidami area, Central Eastern Desert, Egypt.

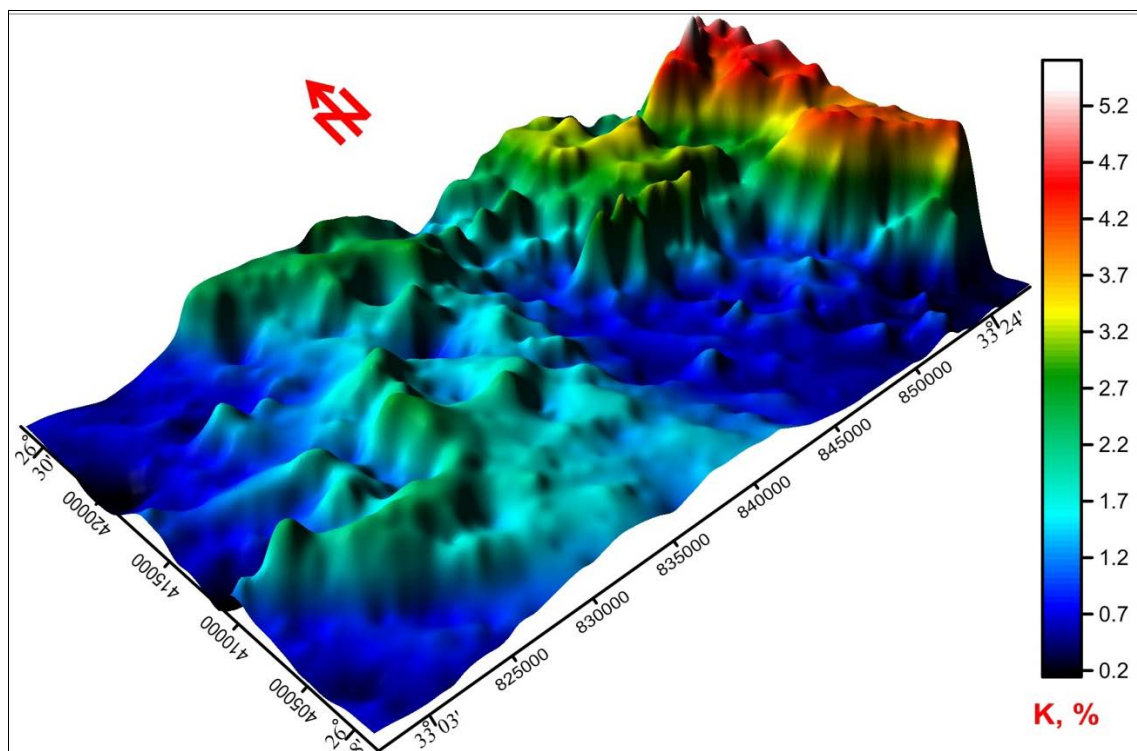


Fig. (9): Airborne K (%) 3D image map of Wadi Elgidami area, Central Eastern Desert, Egypt.

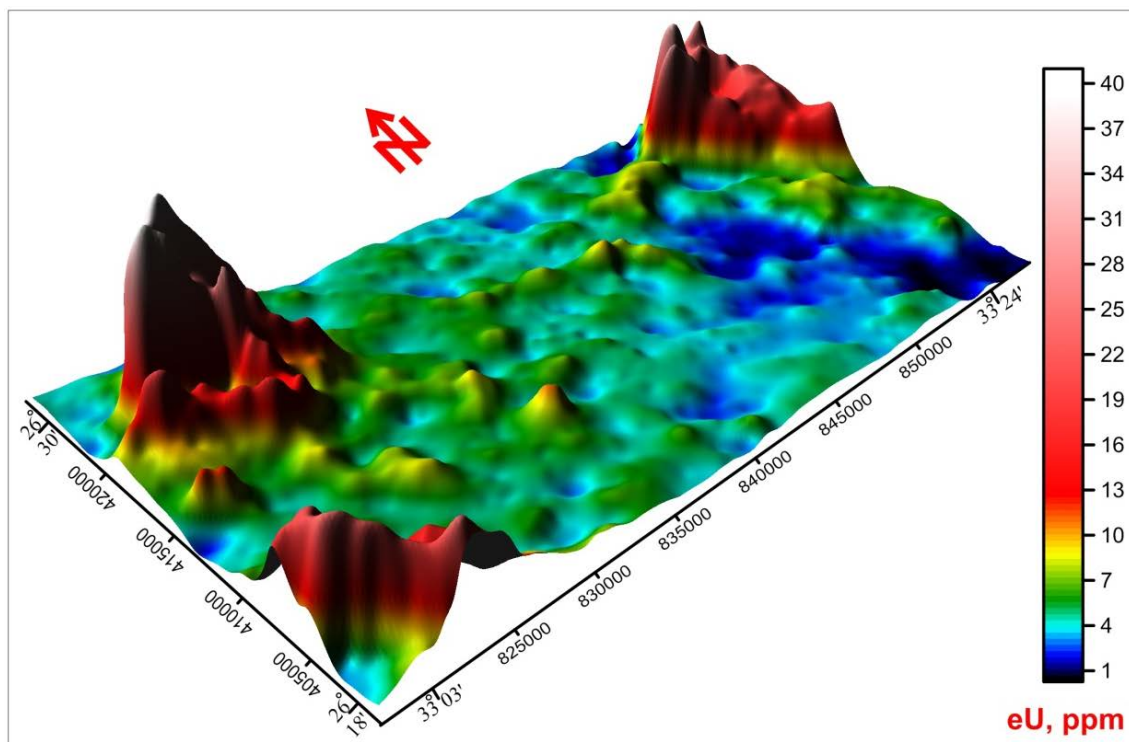


Fig. (10) Airborne eU (ppm) 3D image map of Wadi Elgidami area, Central Eastern Desert, Egypt.

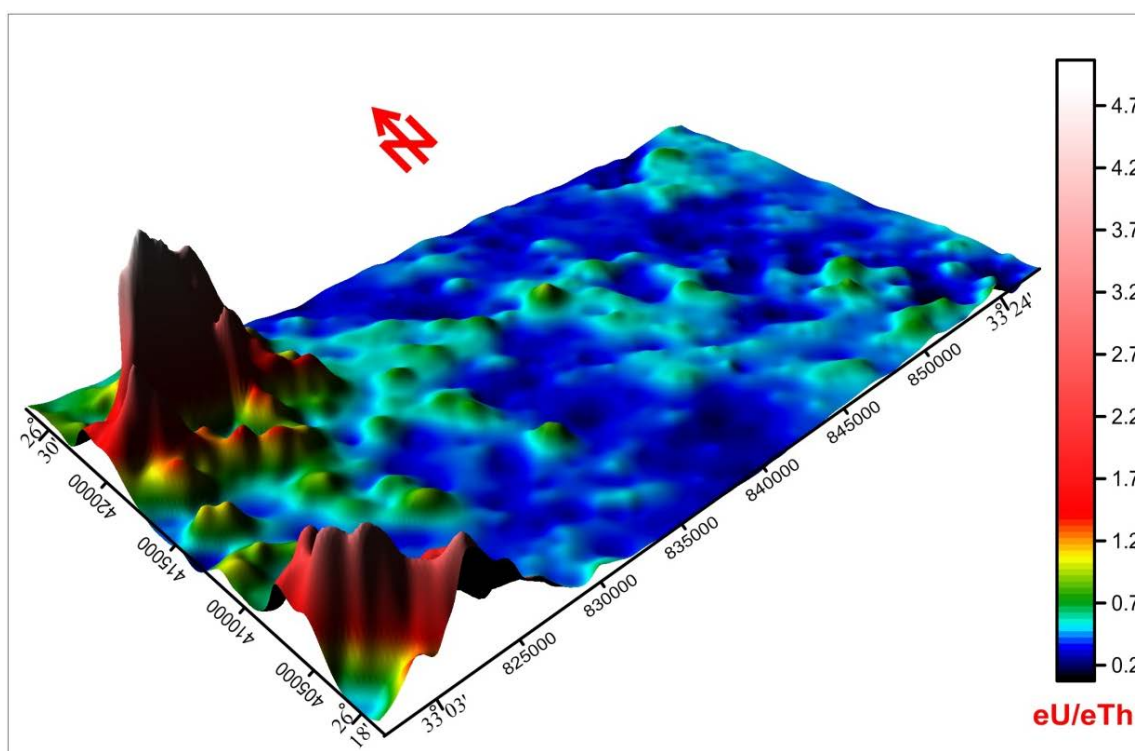


Fig. (11) Airborne eU/eTh ratio 3D image map of Wadi Elgidami area, Central Eastern Desert, Egypt.

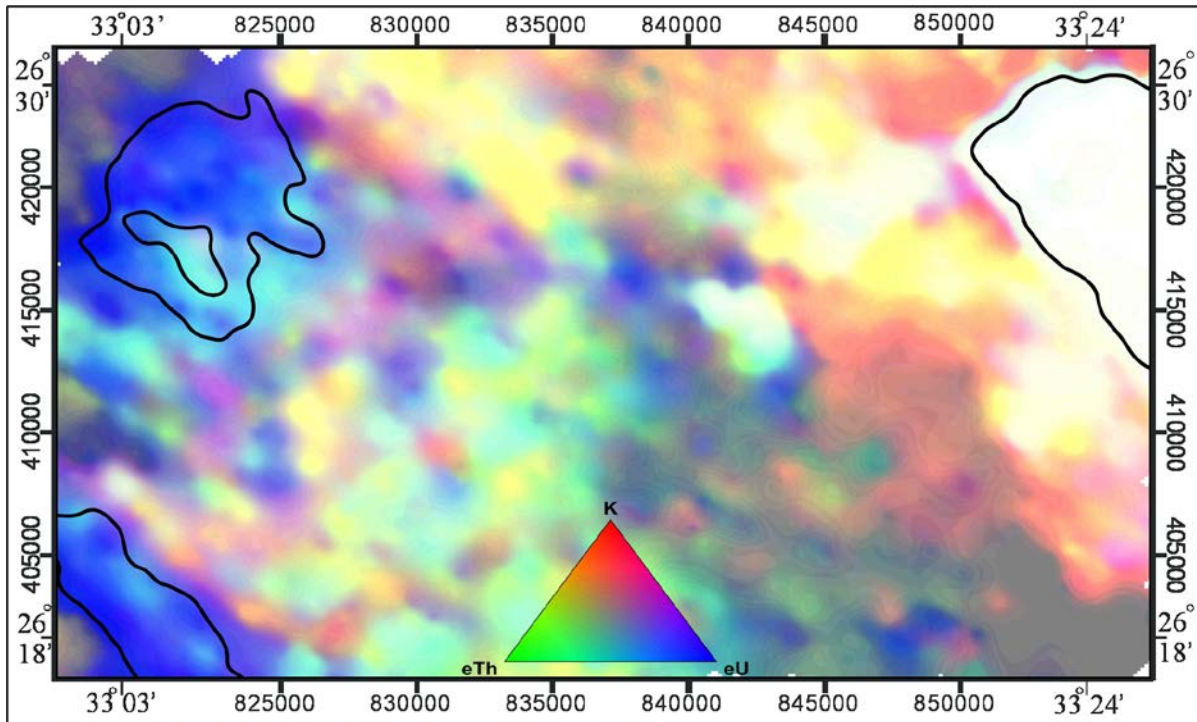


Fig. (12) Airborne eU, eTh and K composite image map of Wadi Elgidami area, Central Eastern Desert, Egypt.

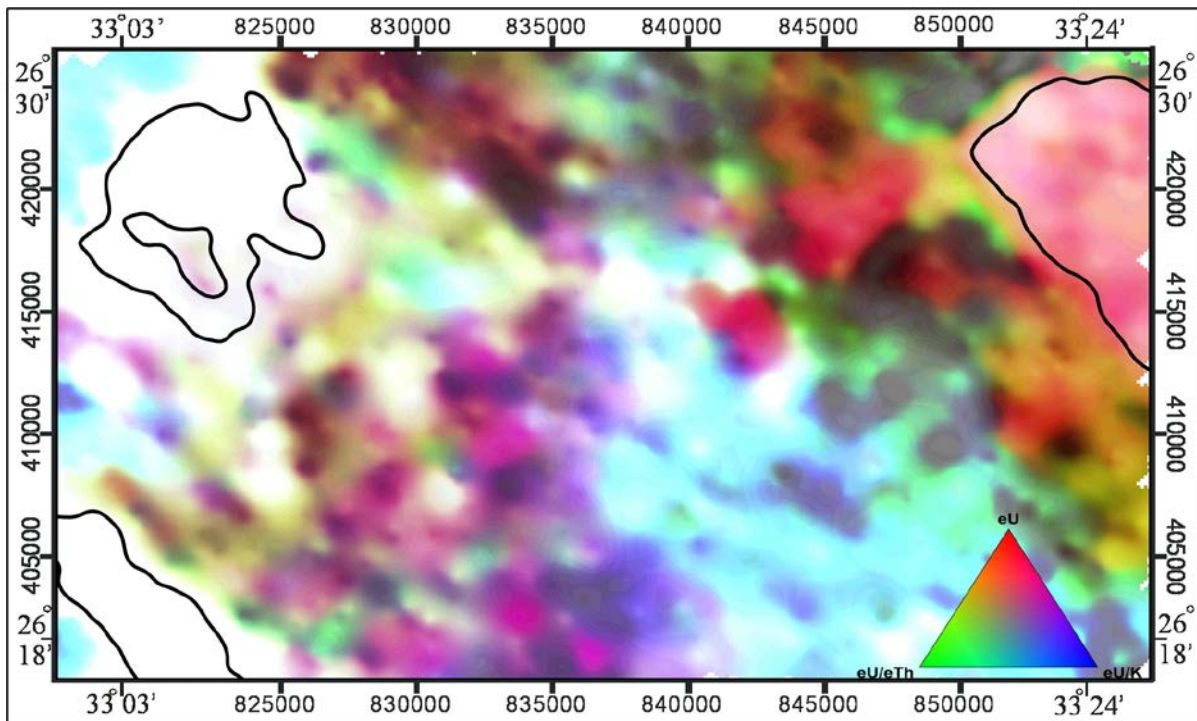


Fig. (13) Airborne eU, eU/eTh and eU/K composite image map of Wadi Elgidami area, Central Eastern Desert, Egypt.

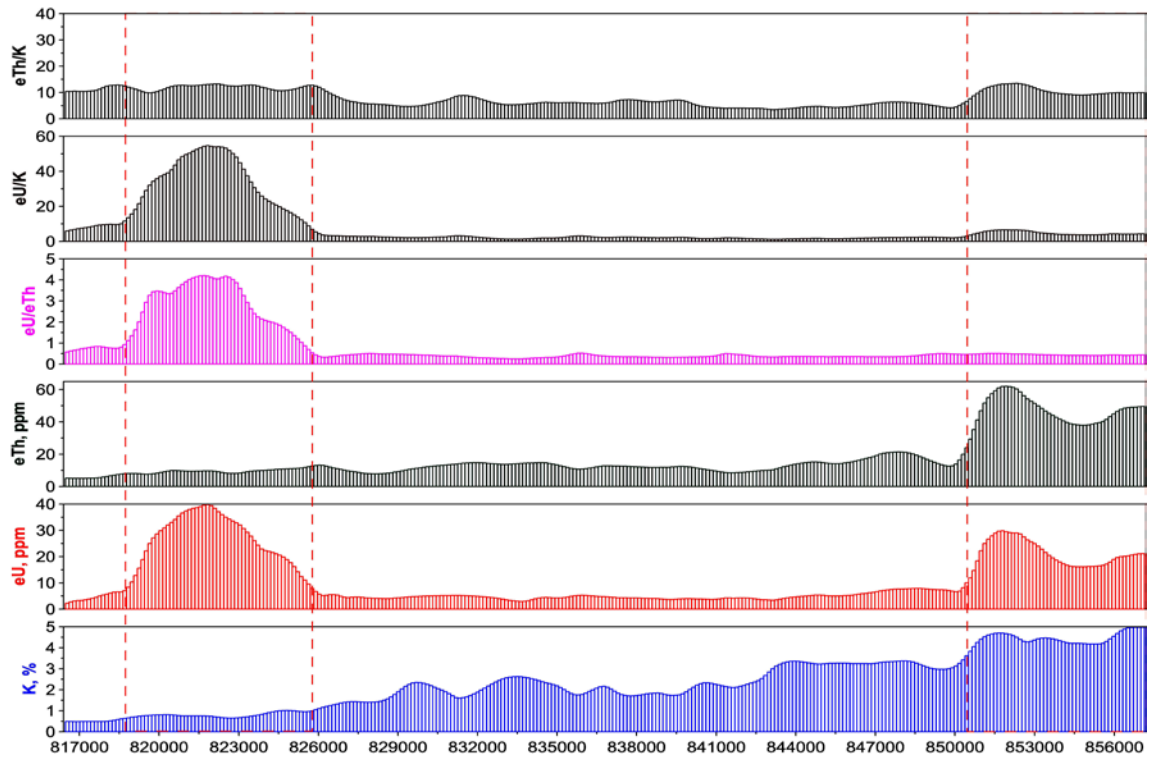


Fig. (14): Airborne radioelement stacked profiles in the SW-NE direction of Wadi Elgidami area, Central, Eastern Desert, Egypt.

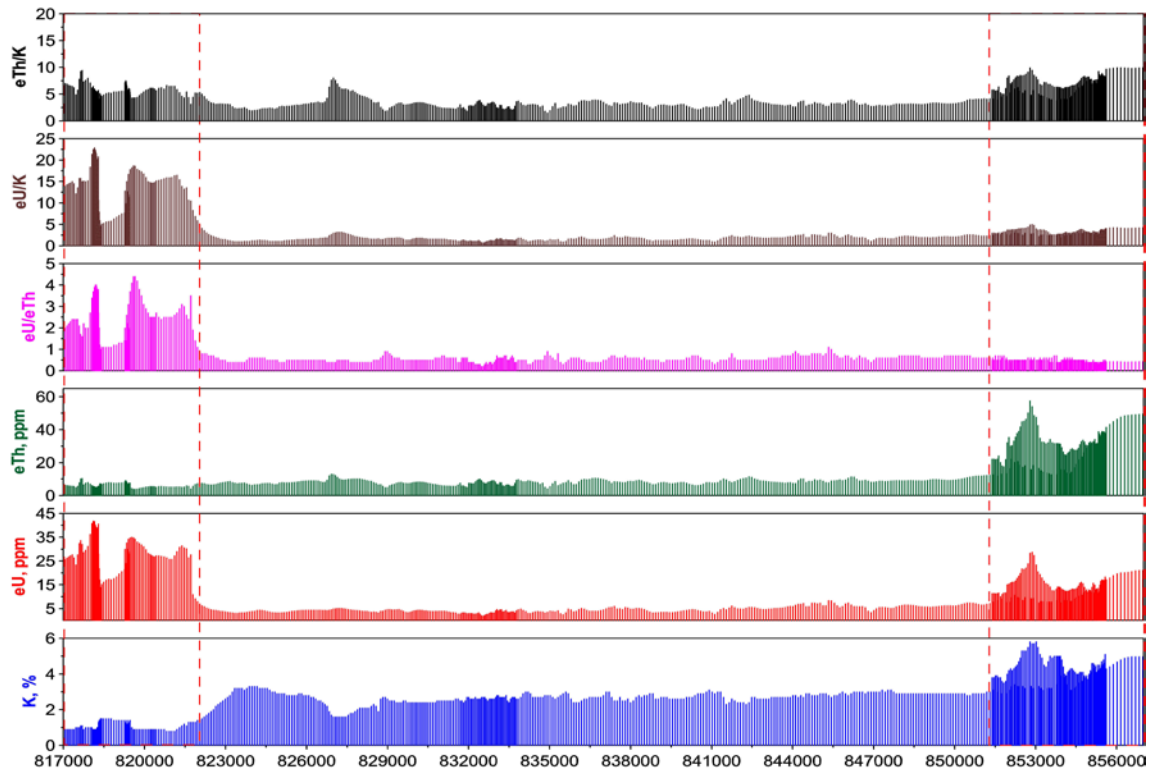


Fig. (15): Car-borne radioelement stacked profiles in the SW-NE direction of Wadi Elgidami area, Central, Eastern Desert, Egypt.

Younger granites show red colour, which means that they contain relatively high concentrations of uranium, but they contain low values for eU/eTh and eU/K and this, reduces its importance as a source of uranium. The rest of the rock units do not represent any significant increases in radioactivity levels, but are distinct from each other subtly. Red colour is predominant than green and blue in the case of older granites. Taref formation is distinguished by the predominance of greener colour than the red and blue colours. Meanwhile, blue is predominant over red and green in the case of Dawi formation.

6.3. Stacked Profiles

A profile was drawn crossing the study area from southwest to northeast to study clarify, and compare both the airborne and car-borne gamma-ray spectrometric survey results (Figs. 14 & 15). Very high agreement was found between both of them. Potassium profile reached its highest value (5 %) coinciding with younger granites, and then decrease gradually in the southwestern direction to less than 0.5%. eU profile is characterized by the existence of two anomalies, one of them is located in the direction of the northeast and related to younger granites reaching 25 ppm. Meanwhiles the other anomaly, in the direction of the southwest and is associated with phosphate beds of Dakhla formation, reaching 40 ppm eU. The remaining rock units in the study area show nearly the average background of the three elements in the earth crust. The profile of eTh shows the presence of only one anomalous zone of up to 60 ppm that is related to younger granites, located in its northeastern part of the study area. Then, suddenly lower values do the rest of rock units in the southwestern direction of the study area. Meanwhile, each of eU/eTh and eU/K ratios profiles possess high anomalies up to 4 ppm/ppm and 55 ppm/% respectively in the southwestern part of the study area, associated with Dakhla formation and its phosphate beds. The eTh/K ratio profile does not represent any clear anomaly in the study area, but all rock units are approximate.

7. CONCLUSIONS

High-sensitivity airborne spectrometric survey represented a useful tool for mapping surface geology of the study area. The composite image technique was applied to these data to facilitate the correlation and delineation of lithologic units based on subtle differences in the radioelement concentrations and ratios. The method showed a practical success to map basement- sedimentary contact, delineate and subdivide various rocks in the study area.

Reviewing the results of airborne and car-borne spectrometric surveys shows a high agreement between the resultant radioelement distribution maps of both of them. The resultant data indicate the association of Elmissikat younger granites with the highest levels of both eTh and K in the study area up to 60 ppm and 5.5% respectively, as well as high concentrations of eU up to

30 ppm. The western part of the study area is characterized especially phosphate-rich rocks of Dakhla formation that contain high concentrations of uranium up to 42 ppm. Meanwhile, they represent the lowest level for each of the eTh and K concentrations in the study area. The remaining rocks of the study area, which includes older granites, metavolcanics and ophiolites as well as the rest of sedimentary formations are free of any high concentrations in any of the three radioactive elements.

The present study recommends a detailed ground study for the northwestern part of the study area, which represents the highest content of eU. This study includes conducting semi-detailed and detailed ground geophysical and geochemical surveys, and collecting representative samples for analyses to this important part that is believed to represent significant phosphate beds.

Acknowledgment

Deep thanks from the authors to Dr. Tarek Ibrahim, Head of Remote Sensing Department, for his help and support during field work. Grateful thanks are also extended to Prof. Dr. Ahmed A. Ammar, Exploration Division, Nuclear Materials Authority, for his revision and fruitful discussions.

REFERENCES

- Aero Service, 1984**, Final operational report of airborne magnetic/radiation survey in the Eastern Desert, Egypt. Aero-Service Division, Houston, Texas, USA, Six Volumes.
- Aissa, M. and Jubeli, Y. M. 1997**, Carborne gamma-ray spectrometric survey of an area east of Homs, Central Syria. Applied Radiation and Isotopes, Vol48, PP.135-142.
- Ammar, A.A. (1973)** Application of Aerial Radiometry to the Study of the Geology of Wadi El- Gidami, Eastern Desert, Egypt, (with aeromagnetic application), Ph. D. Thesis, Faculty of Science, Cairo University, Geiza, Egypt, p. 424.
- Anderson, H. and Nash, C., 1997**, Integrated lithostructural mapping of the Rossing area, Namibia using high resolution aeromagnetic, radiometric, Landsat data and aerial photographs, Exploration Geophysics, Vol28, PP.185-191.
- Charbonneau, B.W., Holman, P.B. and Hetu, R.J., 1997**: Airborne gamma spectrometer magnetic-VLF survey of northeastern Alberta. Geological Survey of Canada Bulletin Vol 500, PP.107-132.
- Conoco Inc., 1989**, Stratigraphic lexicon and explanatory notes to the geological map of Egypt 1:500,000. Conoco Inc., Cairo, Egypt, , 262p.
- Cook, S.E., Corner, R.J., Groves, P.R. and Grealish, G.J., 1996**, Use of airborne gamma radiometric data for soil mapping. Aust. J. Soil Res., Vol 34, PP.183-194.

- Duval, J.S., 1983**, Composite color images of aerial gamma-ray spectrometric data, *Geophysics*, Vol48, PP. 722- 735.
- Ford, K.L., Savard, M., Dessau, J. C. and Pellerin, E., 2001**, The role of gamma-ray spectrometry in radon risk evaluation: A case history from Oka, Quebec. *Geoscience Canada*, Vol. 28, 2P.
- Gaafar, I. M. 2005**: Applications of geological and geophysical survey for defining the uranium potentiality of some younger granites in the Eastern Desert of Egypt. Ph D Thesis Fac. of Sc., Mansoura, Univ., Egypt 180 p.
- Ghanem, M., Zalata, A., Abd El- Razik, T., Mikhailov, I., Razraliaev, A. and Mirtov, Y., 1970**, Stratigraphy of the phosphate-bearing Cretaceous and Paleocene sediments of the Nile Valley between Idfu and Qena. *Studies on some mineral deposits of Egypt. UAR Geol. Surv.*, Article 7, p. 109 – 134.
- Glenn, C.R. and Mansour, S.E.A.,1979**, Reconstruction of the depositional and diagenetic history of phosphorites and associated rocks of Duwi Formation (Late Cretaceous) Eastern Desert, Egypt. *Geol. Surv.*, VolVIX ,pp 388-407.
- Graham, D.F. and Bonham-Carter, G.F., 1993**, Airborne radiometric data: a tool for reconnaissance geological mapping using a GIS. *Photogrammetric Engineering and Remote Sensing*, Vol58, PP.1243-1249.
- Grasty, R.L.and Cox, J.R., 1997**: A carborne gamma-ray spectrometer system for natural radioactivity mapping and environmental monitoring. In: Hovgaard, J. (ed.). *Rapid Environmental. Surveying Using Mobile Equipment*, NKS, ISBN87-7893-014-6.
- Grasty, R.L. and Shives, R.B.K., 1997**, Applications of gamma ray spectrometry to mineral exploration and geological mapping, Aworkshop Presented at Exploration 97: Fourth Decennial Conference on Mineral Exploration.
- Hjerpe, T., Finck, R.R. and Samuelsson, C., 2001**, **Statistical data evaluation in mobile gamma spectrometry**; an optimization of on-line search strategies in the scenario of lost point sources. *Health Phys* Vol80 (6), PP. 563-570.
- Hovgaard, J. (Ed.), 1997**, *Rapid environmental surveying using mobile equipment*. Nordic Nuclear Safety Research, Copenhagen, ISBN87-7893-014-6
- IAEA, 2010**: radioelement mapping. IAEA nuclear energy series no. nf-t-1.3. International atomic energy agency, Vienna, 2010, 123 P.
- Ibrahim, T. M., 2002**, Geologic and radioactive studies of the basement-sediment contact in the area west Gabal El-Missikat, Eastern Desert, Egypt. Ph. D. Thesis, Faculty of Science, Mansoura University, Mansoura, Egypt.
- Jaques, A.L., Wellman, P., Whitaker, A.and Wyborn, D., 1997**, High resolution geophysics in modern geological mapping. *AGSO Journal of Australian Geology & Geophysics*, Vol 17, PP. 159-174.
- Karlsson, S., Mellander, H., Lindgren, J., Finck, R.R.and Lauritzen, B. (Eds.), 2000**, resume99 *Rapid environmental surveying using mobile equipment*. NKS-15, ISBN87-7893-065-0.
- Lahti, M., Jonsen, D.G., Multala, J.and Rainey, M.P., 2001**, Environmental applications of airborne radiometric surveys. *Expanded Abstracts, 63rd Annual Conference, European Association of Geoscientists and Engineers*.
- Lo, B.H.and Pitcher, D.H., 1996**, A case history on the use of regional aeromagnetic and radiometric data sets for lode gold exploration in Ghana. *Annual Meeting Expanded Abstracts, Society of Exploration Geophysicists*, PP.592-595.
- Moreira, M.C.F., 1991**, Radiological survey of Goiania by a mobile monitoring unit. *Health Phys* Vol. 60, PP. 81–86.
- Raghuwanshi, S.S. 1992**, Airborne gamma-ray spectrometry in uranium exploration. *Adv. Space Res.* , Vol. 12, PP. 77-86.
- Sanderson, D.C.W., Allyson, J.D. and Tyler, A.N., Scott, E.M., 1995**, Environmental applications of airborne gamma-ray spectrometry,IAEA-TECDOC-827, IAEA, Vienna,Austria PP. 71-79.
- Sanderson, D.C.W., Cresswell, A.J.and Lang J. J. (Eds.), 2003**, An international comparison of airborne and ground based gamma ray spectrometry. University of Glasgow, Glasgow, Scotland, UK, ISBN08-5261-783-6.
- Said, R., 1962**, *The geology of Egypt*. Elsevier, 377 p.
- Tauchid, M.and Jubeli, Y. 1991, Uranium exploration in Syria. SYR/86/005, Terminal Report, IAEA, Vienna,Austria,
- Ulvsand, T., Finck, R.R.and Lauritzen, B. (Eds.), 2002**, Barents Rescue 2001 LIVEX. NKS-54, ISBN87-7893-108-8.
- Wilford, J.R., Bierwirth, P.N.and Craig, M.A., 1997**, Application of airborne gamma-ray spectrometry in soil/regolith mapping and applied geomorphology, *AGSO Journal of Australian Geology and Geophysics*, Vol. 17, PP. 201-216.